

## Chlorophyll increase due to internal waves on the shelf break of Gran Canaria (Canary Islands)\*

P. SANGRÀ<sup>1</sup>, G. BASTERRETXEA<sup>2</sup>, J.L. PELEGRÍ<sup>1</sup> and J. ARÍSTEGUI<sup>1</sup>

<sup>1</sup>Facultad de Ciencias del Mar, Universidad de Las Palmas de Gran Canaria, 35017 Las Palmas de Gran Canaria, Islas Canarias.

<sup>2</sup>IMEDEA (CSIC-UIB), Miquel Marqués 21, 07190 Esporles, Islas Baleares.

**SUMMARY:** This paper shows observational evidence of internal wave generation and mixing in the southwest shelf-break region of Gran Canaria Island. Signals of periodic internal motion and related mixing events were detected through large pycnocline variations and subcritical gradient Richardson events. Broad areas of homogeneous dense water over the slope, where the vertical temperature field displays a wave-like pattern, provide further evidences of internal wave mixing in this region. The observed diapycnal chlorophyll transport matches with mixing events, suggesting a periodic nutrient supply to the euphotic zone through internal wave mixing. We postulate that internal wave mixing may be an important mechanism contributing to the biological enhancement reported southwest of Gran Canaria Island.

*Key words:* internal waves, chlorophyll, island mass effect, Gran Canaria.

### INTRODUCTION

The increase in biological production around oceanic islands as a consequence of the perturbation of oceanic and atmospheric flows is known as the "island mass effect". Some examples of this phenomena are those reported in the Hawaiian Islands (Gilmartin and Revelante 1974), Mare and New Caledonia Islands (Le Borgne *et al.*, 1985), Prince Edward Island (Boden and Parker, 1986; Perissinotto and Duncombe Rae, 1990) and Aldabra Island (Heywood *et al.*, 1996). Eddies on the leeward side of the island, vertical mixing on the island shelf, benthic nutrient generation, seepage from terrestrial sources and internal waves

have been proposed as the main mechanisms responsible for the island mass effect.

Relatively high productivity and biomass values were observed on the southwest coast (leeward side) of Gran Canaria (Canary Islands), where the shelf is relatively wide. In particular, Hernández-León (1991, 1988) reported mesozooplankton biomass values up to ten times higher on the lee shelf of Gran Canaria than those observed for typical oceanic waters around the Archipelago. He postulated that such biomass enhancement resulted from an increase in biomass at the flanks of the island, related to an increase in primary production during wind pulses (Arístegui *et al.*, 1988), and its subsequent advection toward the island wake where the organisms accumulate.

Upwelling filaments radiating from the African coastal upwelling region and cyclonic and anticy-

\*Received May 4, 2000. Accepted September 28, 2000.

clonic eddies generated leeward of the islands are quite common features around Gran Canaria. These features are largely responsible for the plankton biomass distribution in oceanic waters (Aristegui *et al.* 1994, 1997; Barton *et al.* 1998; Barton *et al.*, 2001). Cyclonic eddies could contribute to the plankton biomass enhancement on the island's wake shelf, through the advection of biomass generated by the eddy dynamics on the island's west flank. Anticyclonic eddies could also export biomass toward the island's wake shelf from the island's east flank or from African upwelling filaments (Aristegui *et al.*, 1997; Barton *et al.*, 1998). In this paper, we explore the possibility that internal wave mixing may be another mechanism responsible for the biological enhancement observed in the shelf waters of Gran Canaria.

The enhancement of biological productivity in some shelf-break regions has been attributed to internal tide mixing, which induces upward transport of nutrient-rich cool water (Pingree *et al.*, 1986; New and Pingree, 1990; Mann and Lazier, 1991). This process not only affects the pelagic system but may also influence benthic communities (Pineda, 1994, 1995; Leichter *et al.*, 1996). The interaction of the surface tide with the steep shelf break topography may generate packets of internal waves travelling away from the shelf break (Prinsenber and Rattray, 1975; Prinsenber *et al.*, 1974; Baines, 1982; New, 1988; New and Pingree, 1990). The energy of internal tides propagates upward (inshore and/or offshore) from the shelf break, along characteristic ray paths. Energy rays, characterized by regions of large vertical oscillations, may cross the thermocline several times after reflection from the bottom or at the surface, leading to inverted V-shaped mixing regions at either side of the shelf-break (e.g. Fig. 5 of New and Pingree, 1990). This mixing would build up cores of homogeneous dense water over the shelf-break region, providing conditions favourable to biological enhancement through upward nutrient transport.

A physical and biological survey was carried out in the shelf break region southwest of Gran Canaria Island, from October 25 to November 5 1994, to investigate the effect of internal waves on the phytoplankton abundance and distribution. The northeast propagation of the surface tide, the lack of wind mixing, and the steep shelf break topography of this region suggested that the increase in biological productivity there could be related to the generation of internal waves at the shelf break. For this reason the

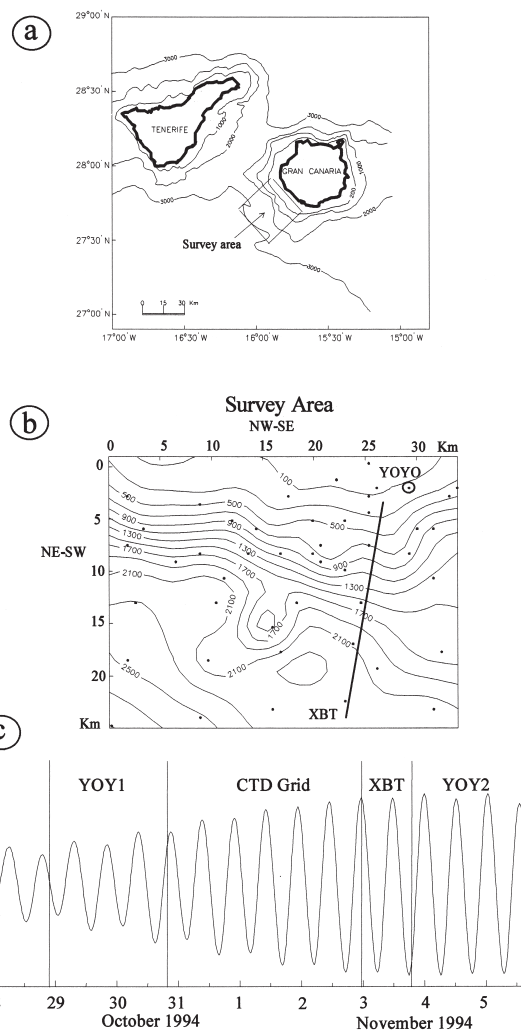


FIG. 1. – (a) Central region of the Canary Archipelago and area of study. (b) Survey area bathymetry, depth contours are marked in meters, the dots indicate CTD stations, the solid line indicates the fast XBT transect, and circle dot shows the position of the fixed sampling location. (c) Survey legs with superimposed barotropic tide amplitude.

survey focused on detecting the signal of such internal motion and its biological effect. The present work represents, to our knowledge, the first observational evidence of internal wave generation and mixing over the slope of Gran Canaria.

## SURVEY

The survey area was located on the slope southwest of Gran Canaria (Fig. 1a). The bathymetry of the area consist of a steep insular slope where the sea-floor raises abruptly from 2000 to 100 m in less than an average horizontal distance of 10 km (Figure 1b). The survey was planned along four different legs with the aim of detecting both the spatial and

temporal signals of internal motion (Fig. 1c). First, during a neap tide period, a repeated sampling (hereafter YOY1) was carried out on board *R/V Taliarte* at a fixed point near the shelf break (Fig. 1b). Density and velocity profiles were obtained hourly during three tidal cycles using an ME conductivity-temperature-depth (CTD) probe that incorporated an acoustic doppler currentmeter. The main objective of this first sampling was to detect internal motions through pycnocline oscillations. In a second leg a 45 CTD stations grid was sampled, covering the slope region, with the purpose of detecting regions of enhanced mixing associated with the presence of internal waves. This sampling was followed by a fast expendable bathythermograph (XBT) transect crossing the slope, which provided a nearly instantaneous picture of the water column and allowed the observation of the spatial signal of internal motions (Fig. 1b). Finally, a second time series was done at the same location as YOY1, with samples every hour during four tidal cycles of a spring tide (hereafter YOY2) (Fig. 1c).

A parallel sampling, carried out at the same shelf-break point on board *R/V Monachus*, started three days before YOY1 and lasted almost until the end of YOY2 (hereafter YOYM). Hourly CTD and fluorescence profiles were obtained at a single station with a Seacat-19 CTD that incorporated a Sea-Tech fluorometer. Water samples, collected with a Niskin bottle, were used for chlorophyll analysis in order to calibrate the fluorescence probe. For this purpose, 250 ml subsamples were filtered through Whatman GF/F glass fibre filters. Chlorophyll was extracted in 10 ml of 90% acetone overnight at 4°C and measured in an on-deck Turner Designs fluorometer calibrated with pure chlorophyll-a. Simultaneous sampling using both CTDs on board *R/V Taliarte* and *R/V Monachus* was done for intercalibration purposes.

## TEMPORAL SIGNAL OF INTERNAL WAVES

The time series evolution of the pycnocline structure, as obtained from YOY1 casts, is displayed in Figure 2a. Above the pycnocline, centred at 80 meters, a mixed layer develops with an average depth of 60 meters. The temporal evolution of the pycnocline clearly shows vertical oscillations with maximum amplitudes of up to 30 meters. Although the oscillations seem to have a non-linear behaviour, there seems to be some coupling with the barotrop-

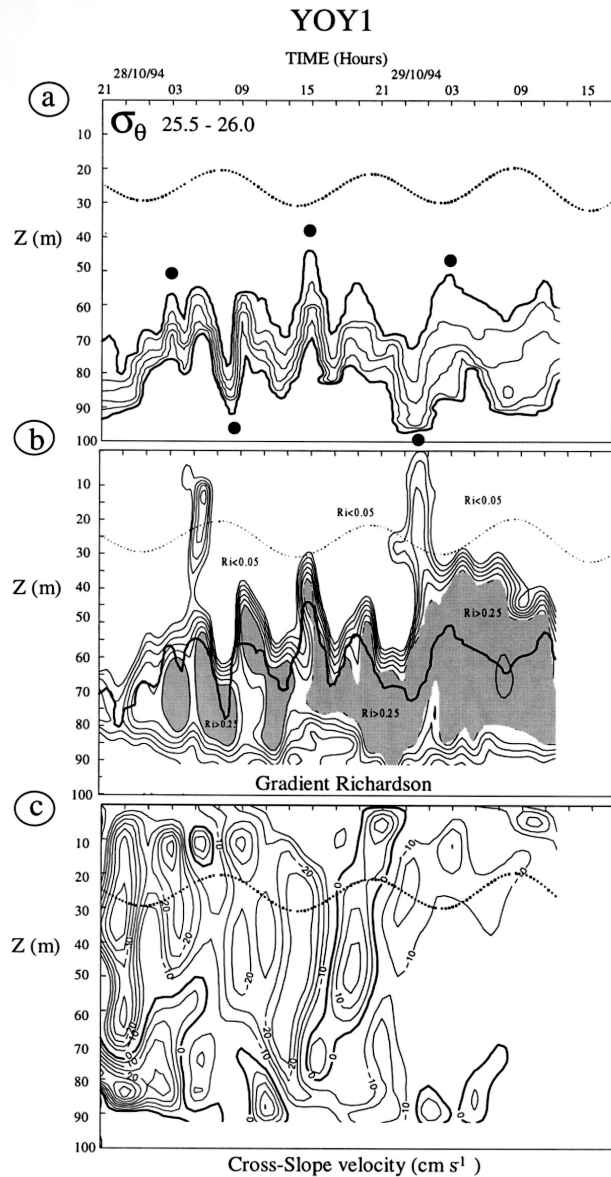


FIG. 2. – (a) Sigma theta, (b) gradient Richardson number, and (c) cross-slope velocity contours recorded from YOY1 time series. In (a) the isopycnals bounding the pycnocline (25.5 and 26.0) are marked with bold contours and the coincidence between the barotropic tide and the pycnocline oscillations is emphasized with black dots. In (b) the shaded areas indicate supercritical gradient Richardson values ( $<0.25$ ) while the bold line shows the 25.5 isopycnal. In (c) the positive and negative values represent northeasterly and southwesterly flow respectively, and bold contours represent the zero velocity value. In all parts the wave-like dotted line represents the amplitude of barotropic tide.

ic tide. In general, the pycnocline crests are coincident with barotropic troughs whereas the pycnocline troughs coincide with barotropic tide crests (barotropic crests and troughs are indicated with a dot in Figs. 2a and 3a). This suggests a baroclinic internal tide mode with a semidiurnal period. Nevertheless, secondary crests and troughs with short

periods (about 6 hours) were also detected. Studies of internal tide generation in other shelf break regions have related the presence of such high frequency components to non-linear and dispersion processes (Pingree *et al.*, 1986; New and Pingree, 1990). The same pattern is also observed in the YOY2 time series (Fig. 3a), where pycnocline crests/troughs are closely related to barotropic tide troughs/crests and a signal of high frequency oscillations is also present.

A close look at the temporal structure of the pycnocline reveals that during certain periods the diapycnal distance increases considerably, suggesting the occurrence of mixing processes. Figures 2b and 3b show the temporal evolution of the gradient Richardson number, defined as

$$Ri = \frac{N^2}{(\partial u / \partial z)^2 + (\partial v / \partial z)^2}$$

where  $u$  and  $v$  are the horizontal components of velocity,  $z$  is the vertical coordinate (positive upwards) and  $N$  is the Brunt-Väisälä frequency ( $N^2 = -(g/\rho) d\rho/dz$ , a function of the density field  $\rho(z)$ ). The profiles of the gradient Richardson number were computed from the density and velocity casts interpolated at every meter. Since the raw velocity data were quite noisy, they were smoothed using a running filter in both the vertical and temporal coordinates. The time-depth  $Ri$  distribution shows the existence of regions in the pycnocline with values falling below a critical number ( $Ri < 0.25$ ), indicating the possibility of vertical mixing through Kelvin-Helmholtz instabilities. The wind intensity during the survey was relatively low (average winds of 2.5 m/s for YOY1 and 3.2 m/s for YOY2), which suggests that the mixing events were not related to wind supplied energy. An alternative energy supply mechanism for mixing is the strong velocity shear associated with the baroclinic character of internal waves. This baroclinic behaviour of the velocity field is clearly noticeable in the temporal evolution of the velocity profiles, mainly during the barotropic troughs, as plotted in Figures 2c and 3c. As an example, during the first barotropic trough of YOY1 (around 03:00 hours, October 29) there was a vertical inversion of the velocity field, southward in the mixed layer and northward in the bottom layer. The kinetic energy of this sheared water column is transformed into potential energy, overcoming gravitational stability and inducing vertical mixing. During YOY2 there also appears to be mixing near all barotropic troughs (Fig. 3b), particularly the last

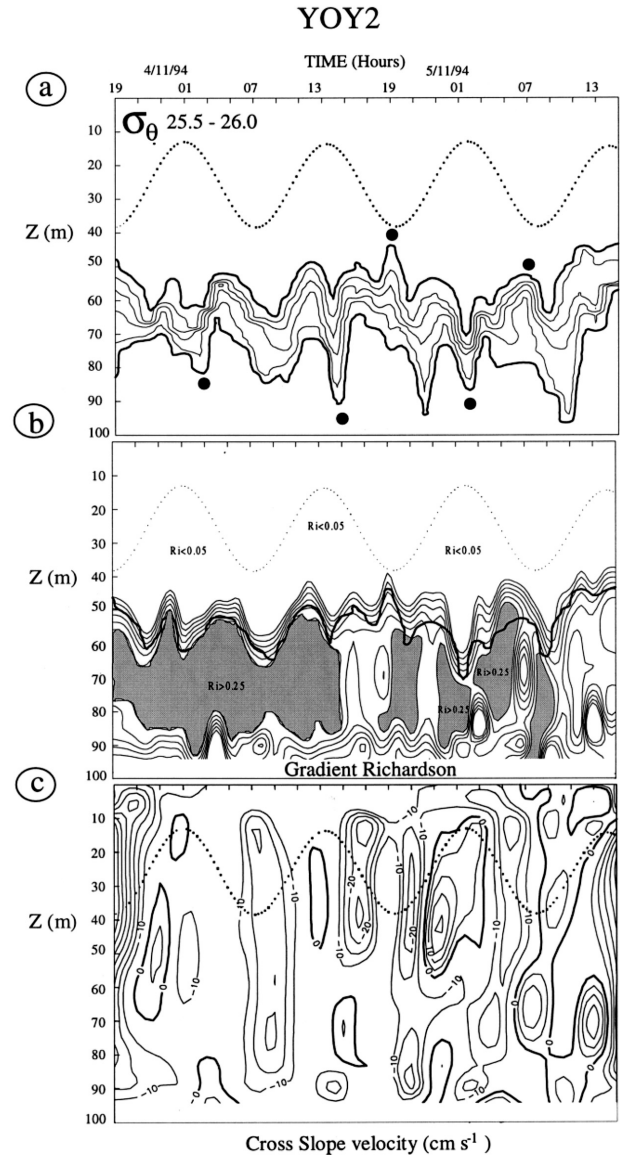


FIG. 3. – Same caption as Figure 2 but for YOY2 time series.

one. Mixing events during barotropic tide troughs have been also reported in other regions where internal tides are generated at the shelf break (New, 1988; New and Pingree, 1990). Since the shelf and slope southwest of Gran Canaria are protected from the Trade winds, it is likely that shear by internal waves is the main mixing mechanism.

The increase in shear related to the barotropic tide troughs may be explained as the result of the interaction between the barotropic tide and the mean currents observed in this area. In the Canary Basin the tidal wave propagates to the northeast, impinging onto the southwest coast of the archipelago islands, in particular Gran Canaria. For this reason, in deep waters the tidal currents mainly flow into the



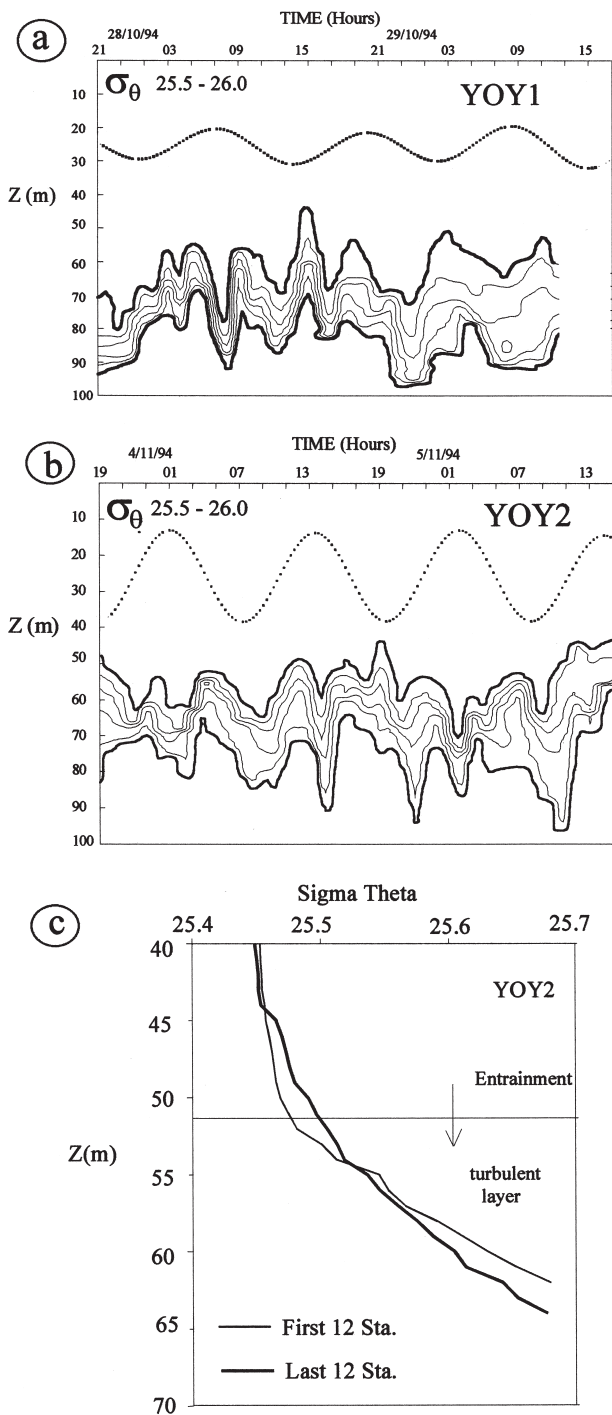


FIG. 4. – Depth and thickness of the pycnocline during (a) YOY1 and (b) YOY2. (c) Averaged density profiles during the first and last twelve casts of YOY2.

southwest (ebbs) or northeast (floods) directions (Siedler and Paul, 1991). The mean near-surface currents, on the other hand, are the result of the southward flowing geostrophic Canary Current and the southwestward flowing Ekman transport, both of

them reaching maximum values near the sea surface. Therefore, during the ebb tide (troughs in the barotropic tide) the mean current adds to the tidal current near the surface, attaining maximum negative (southwestward) values and reaching maximum vertical shear at the seasonal pycnocline. Conversely, at high tides (crests) the mean and tidal currents oppose each other and the resulting near surface current diminishes, causing a decrease in the vertical shear. Such pattern is displayed by the time series velocity profile, with the velocity reaching maximum values (southwesterly) during the barotropic tide troughs and minimum values during barotropic tide crests (Figs. 2c and 3c).

The temporal evolution of the pycnocline reveals two features that are apparently related to internal wave mixing (Fig. 4). First, there is a noticeable increase in the diapycnal distance from YOY1 to YOY2. This suggests that “intrapycnocline” mixing, which results from shear-induced turbulence, is

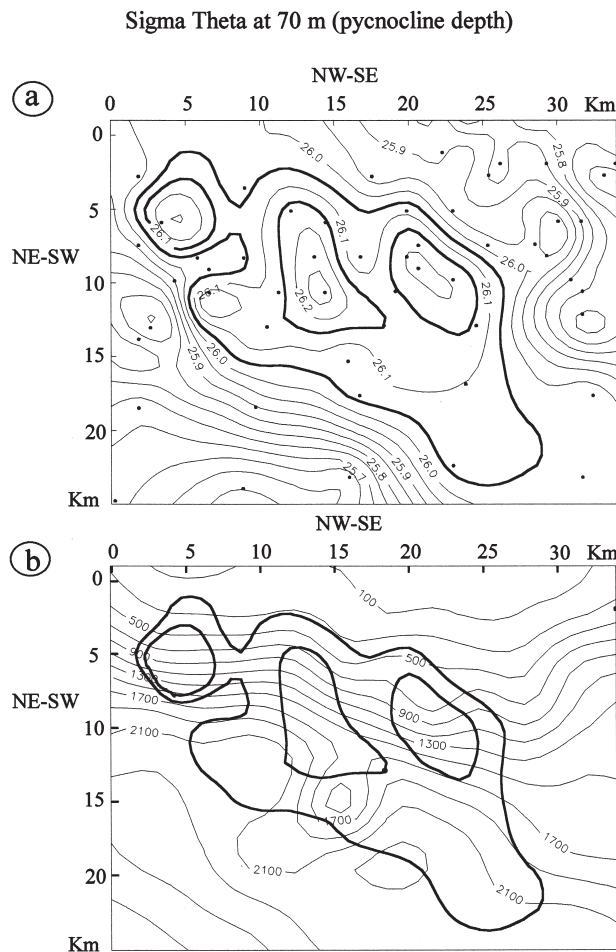


FIG. 5. – (a) Sigma theta contours at 70 m depth as obtained from the CTD grid. (b) The relatively homogeneous dense water (as indicated by the thick lines) is superimposed over the bottom topography.

eroding the pycnocline. Second, from the first to the second time series there is a 15 metre rise in the mean pycnocline depth, which is suggestive of downward fluid entrainment from the upper mixed layer into the pycnocline. This entrainment process has been schematized in Figure 4c, where the averages of the first 12 and last 12 YOY2 profiles have been represented. This one-way entrainment process emphasizes the relative unimportance of wind-induced mixing and suggests the existence of a major turbulence source near the bottom.

### SPATIAL SIGNAL OF INTERNAL WAVES

Figure 5 illustrates the distribution of the potential density field over the southwest insular slope at the mean depth of the pycnocline (70

meters), as obtained from 49 CTD stations. The main feature of the density field is a broad region of relatively homogeneous and dense water (limited by the  $1026,05 \text{ kg m}^{-3}$  isopycnal). This homogeneous high-density region is found over the slope, with several maxima in water density close to the shelf break. This distribution may indicate a source of mixing at the shelf break which progressively extends offshore. As mentioned before, some studies for other shelf-break regions (e.g. New and Pingree, 1990) point out that internal tidal mixing could generate inverted V-shaped mixing regions at either side of the shelf-break, where relatively dense water is transported upward. Hence, the observed homogenisation may be related to mixing by internal waves generated at the shelf break that propagate upwards and offshore.

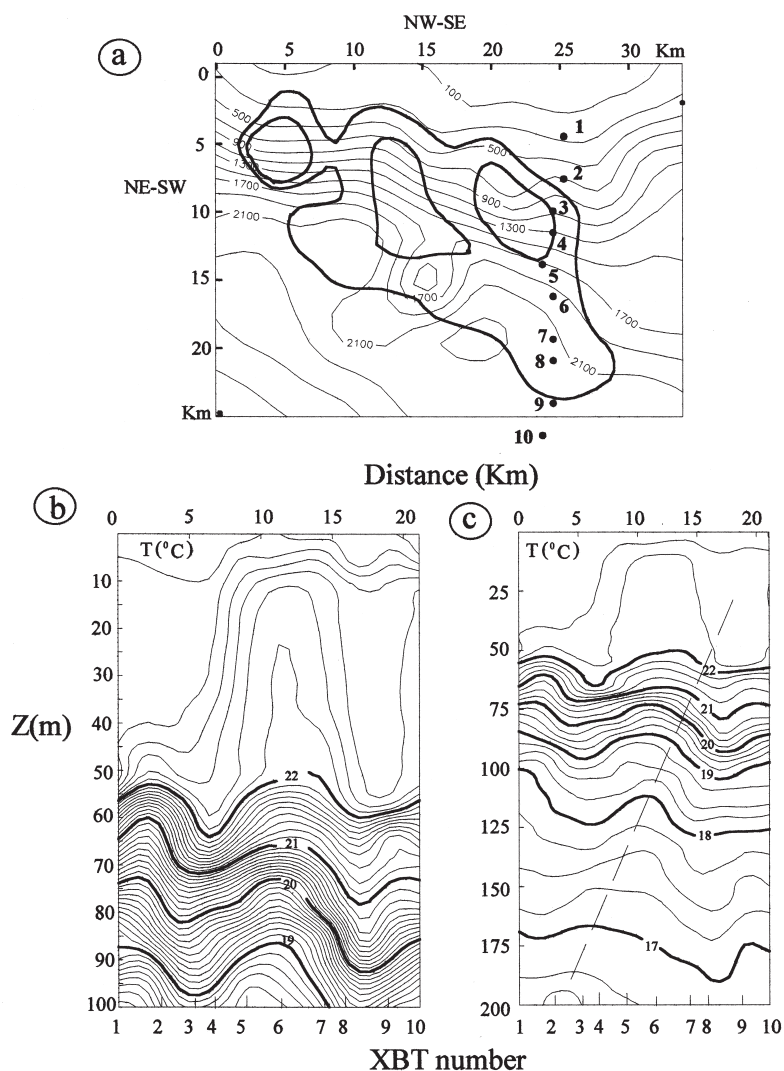


FIG. 6. – (a) Location of the fast XBT section, (b) temperature section down to 100 m, (c) temperature section down to 200 m. In (b) and (c) the bold contours are drawn every 1°C. In (c) the thin broken line joins points of equal phase.

In order to test the above hypothesis, a fast XBT transect (1.5 hours), crossing the relatively homogeneous region was undertaken (Fig. 6a). Figures 6b and 6c show the vertical structure of the temperature field across the relatively homogeneous and dense region, as obtained from the fast XBT transect. The temperature field displays a clear wavelike pattern suggestive of internal motions. The isotherms show vertical oscillations with about 10 m amplitude in the thermocline and 50 m in the mixed layer. In the mixed layer there is also a clear indication of a minimum in gravitational stability. A close look at the wavy isotherm pattern reveals a seaward tilting of constant phase lines. This is clear in Figure 6c, where equal phase points have been joined by a vertical line. If this line is followed from the sea bottom to the sea surface, there is a significant seaward shift of the crests, which suggests that the isothermal

oscillation is due to internal waves propagating upward from the shelf break. This result also reinforces the above argument, that the relatively homogeneous and dense region at the insular slope is due to internal wave-induced mixing.

#### INFLUENCE OF INTERNAL WAVES ON PHYTOPLANKTON DISTRIBUTION

Figures 7 and 8 present the chlorophyll distribution as a function of depth and density as obtained using YOY1, YOY2 and YOYM data. The YOYM fluorometer data have three short temporal gaps and were collected only down to 80 metres. Figures 7b and 8b illustrate the existence of relatively low chlorophyll concentrations in the mixed layer (<0.5 mg m<sup>-3</sup>) and a deep chlorophyll maximum (DCM)

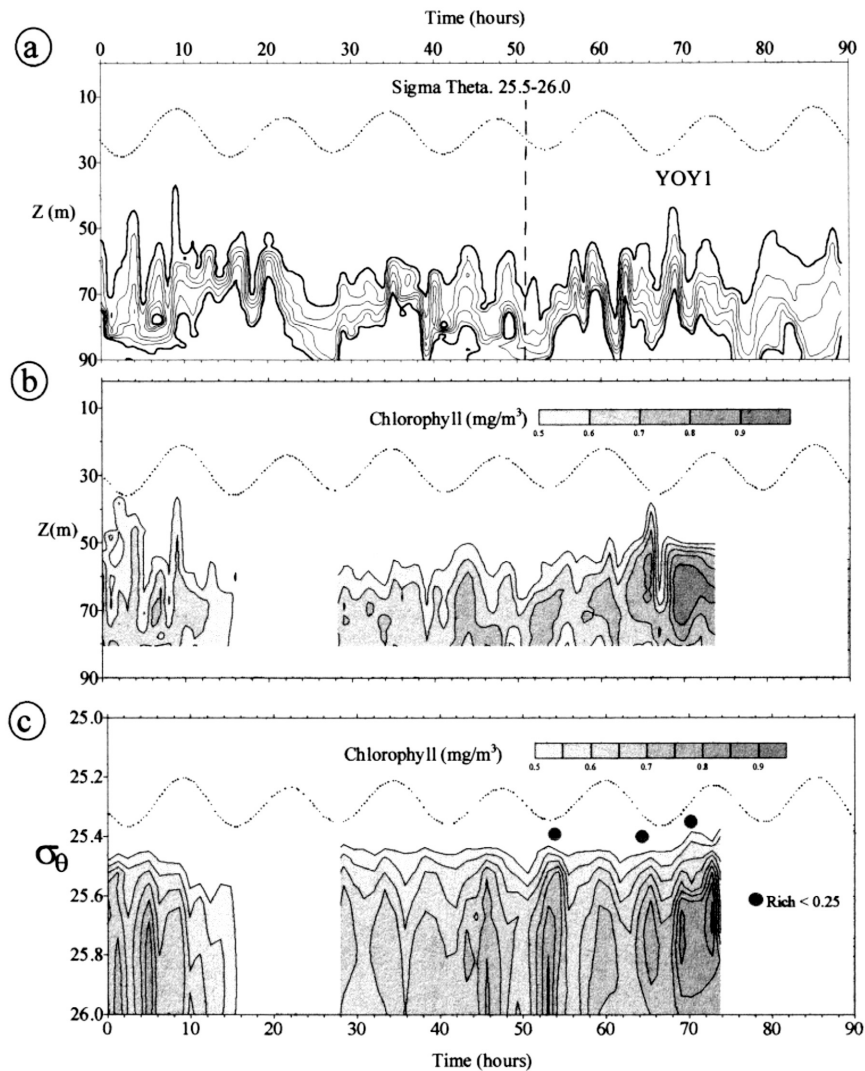


FIG. 7. – (a) Sigma theta and (b) chlorophyll concentration from YOYM time series. (c) Chlorophyll concentration plotted as a function of density, dots correspond to subcritical gradient Richardson regions observed during YOY1.

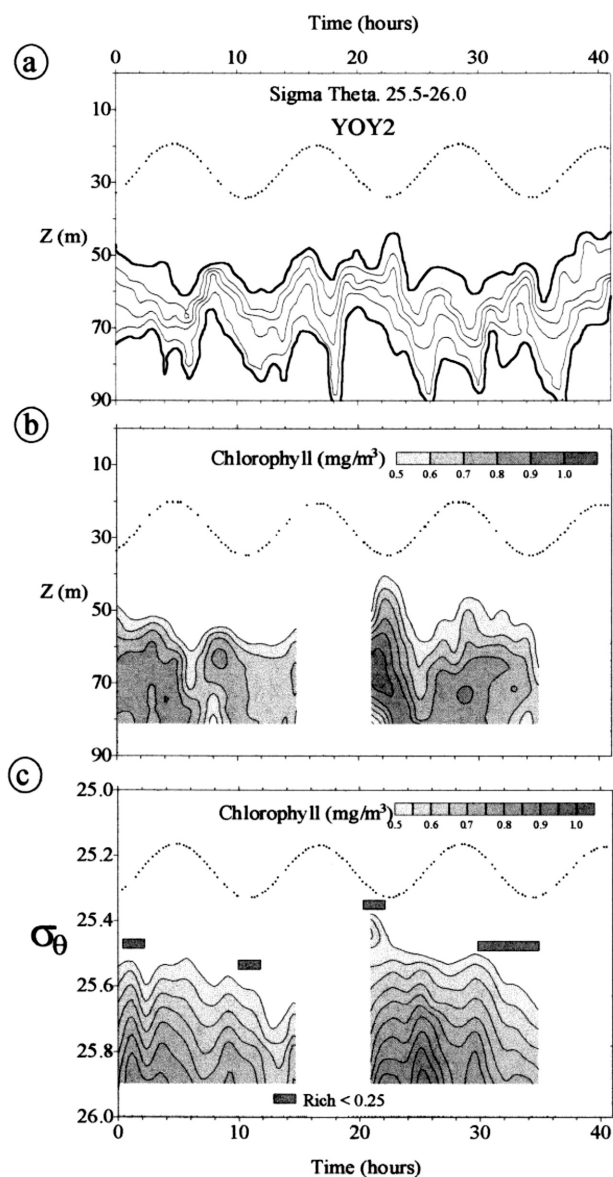


FIG. 8. – (a) Sigma theta and (b) chlorophyll concentration from YOYM time series. (c) Chlorophyll concentration plotted as a function of density, shaded rectangles correspond to subcritical gradient Richardson regions observed during YOY2.

extending down to the seabed. The DCM is clearly associated with the pycnocline and follows its fluctuations. This result suggests the existence of significant coupling between the observed internal waves and phytoplankton dynamics. Depth averaged integrated chlorophyll values (from 5 to 80 m),  $Chl_{int}$ , are  $34 \pm 16 \text{ mg m}^{-2}$ , with little difference between samplings. During some pulses, however, the integrated pigment values increased up to 47% above the average chlorophyll concentrations. Such increases mainly occur during barotropic troughs, when chlorophyll concentrations show pulse-like

enhancements (e.g. Figs. 7b and 8b). This feature is clearly noticeable around the second barotropic trough of YOY1 (hour 66 in Fig. 7b) and the third barotropic trough of YOY2 (hour 22 in Fig. 8b). The biomass increases very rapidly after the barotropic tide trough (1 or 2 hours after the trough). This increase, however, cannot be due to primary production enhancement because of the slow growth rate of phytoplankton (1 doubling per day on average, Parsons, 1980), despite the increase in light availability for raising deep autotrophic cells. A more plausible explanation is the raising of plankton aggregates (high chlorophyll concentrations) as a result of internal wave motion.

In order to relate the appearance of intense diapycnal (cross-isopycnal) phytoplankton transport with internal wave mixing, we plotted the chlorophyll distribution along isopycnal layers (Figs. 7c and 8c). These figures show the intensification of epipycnal (along-isopycnal) chlorophyll gradients during the barotropic troughs, which is indicative of diapycnal chlorophyll transfer. Furthermore, a comparison of the isopycnal chlorophyll distribution (Figs. 7c and 8c) with the gradient Richardson distribution (Figs. 2b and 3b) shows a remarkable correlation between the maxima in chlorophyll concentration and the presence of vertically unstable regions ( $Ri < 0.25$ ). For example, during the last barotropic trough of YOY2 mixing was particularly intense and the chlorophyll distribution displayed a relatively strong epipycnal gradient. The observed matching between subcritical gradient Richardson values and the epipycnal chlorophyll gradients suggests that the increase in biomass during barotropic troughs is associated with upward phytoplankton transport originated through internal wave mixing.

Although nutrients were not sampled, the above results indicate the possibility of periodic nutrient supply from deep layers into the euphotic zone as a result of internal wave mixing. The average pigment concentrations are in the range of values reported by Arístegui (1990) for the shelf of Gran Canaria, about twice the values observed by Arístegui *et al.* (1997) in adjacent surface offshore waters during the same season. This potential role of internal wave mixing is reinforced by the observation of relatively dense homogeneous water over the slope and the absence of significant winds. Although other processes cannot be ignored, we may conclude that internal wave mixing is a potentially important mechanism leading to biological enhancement at the lee of Gran Canaria Island.



## ACKNOWLEDGEMENTS

We are indebted to the captains and crews of the *R/V Taliarte* and the *R/V Monachous* for their assistance in the success of the survey. This research was supported by the Canary Islands government through project OMIAC (91/08 GAC).

## REFERENCES

- Arístegui J., P. Tett, A. Hernández Guerra, G. Basterretxea, M.F. Montero, K. Wild, P. Sangrà, S. Hernández León, M. Cantón, J. García Braun, M. Pacheco, E. D. Barton. – 1997. The influence of island-generated eddies on chlorophyll distribution: a study of mesoscale variation around Gran Canaria. *Deep-Sea Res.*, 44: 71-96.
- Arístegui J., S. Hernández-León, M. Gómez, L. Medina, A. Ojeda and S. Torres. – 1989. Influence of the north trade winds on the biomass and production of neritic plankton around Gran Canaria island. In: Ros J.D. (ed.), *Topics in Marine Biology. Sci. Mar.*, 52(2-3): 223-229.
- Arístegui J. – 1990. La distribución de la clorofila a en aguas de Canarias. *Bol. Inst. es. Oceanogr.*, 6(2): 61-72.
- Baines P.G. – 1982. On internal tide generation models. *Deep-Sea Res.*, 29: 307-338.
- Barton E.D., J. Arístegui, P. Tett, M. Cantón, J. García Braun, Hernández León, L. Nykjaer, C. Almeida, S. Ballesterros, G. Basterretxea, J. Escámez, L. García-Weill, A. Hernández Guerra, F. Lopez-Laatzén, R. Molina, M.F. Montero, E. Navarro Pérez, J.M. Rodríguez, K. van Lenning, H. Vélez, K. Wild. – 1998. The transition zone of the Canary Current. *Progress Oceanogr.*, 41: 455-504.
- Barton E.D., P. Flament, H. Dodds and E.G. Mitchelson-Jacob. – 2001. Mesoscale structures downstream of the Canary Islands. *Sci. Mar.*, 65(Suppl. 1): 167-175.
- Boden B. and L.D. Parker. – 1986. The plankton of the Prince Edward Island. *Polar Biol.*, 5: 81-93.
- Gilmartin M. and N. Revelante. – 1974. The island mass effect, on the phytoplankton and primary production of the Hawaiian islands. *J. exp. Mar. Biol. Ecol.*, 16: 181-204.
- Le Borgne P.J., Y. Dandonneau and L. Lemasson. – 1985. The problem of the island mass effect on chlorophyll and zooplankton standing crops around Mare (Loyalty Islands) and New Caledonia. *Bull. Mar. Sci.*, 37: 450-459.
- Leitcher J.J., S.R. Wing, S.L. Miller and M.W. Denny. – 1996. Pulsed delivery of subthermocline water to Conch Reef (Florida Keys) by internal tidal bores. *Limnol. Oceanogr.*, 41(7): 1490-1501.
- Hernández León S. – 1991. Accumulation of mesozooplankton in a wake area as a causative mechanism of the "island-mass effect". *Mar. Biol.*, 109: 141-147.
- Hernández León S. – 1988. Gradients of mesozooplankton biomass and ETS activity in the wind-shear area as evidence of an island mass effect in the Canary Island waters. *J. Plankton Res.*, 10: 1141-1154.
- Heywood K.J., D.P. Stevens and G.R. Bigg. – 1996. Eddy formation behind the tropical island of Aldabra. *Deep-Sea Res.*, 43: 555-578.
- Mann K.H., and J.R. Lazier. – 1991. *Dynamics of marine ecosystems: Biological-physical interactions in the oceans*. Blackwell Scientific Publications. 466 pp.
- New A.L. and R.D. Pingree. – 1990. Evidence for internal tidal mixing near the shelf break in the Bay of Biscay. *Deep-Sea Res.*, 37: 1783-1803.
- New A.L. – 1988. Internal tidal mixing in the Bay of Biscay. *Deep-Sea Res.*, 35: 691-709.
- Parsons T.R. – 1980. Zooplanktonic production. In: R.S.K. Barnes and K.H. Mann (eds.), *Fundamentals of aquatic ecosystems*. pp. 46-66. Blackwell, Oxford.
- Perissinotto R. and C.M. Ducombe Rae. – 1990. Occurrence of anticyclonic eddies in the Prince Edward Plateau (Southern Ocean): effects on phytoplankton biomass and production. *Deep-Sea Res.*, 37: 777-793.
- Pineda J. – 1994. Predictable upwelling and shore transport of planktonic larvae by internal tidal bores. *Science*, 253: 548-551.
- Pineda J. – 1995. An internal tidal bore regime at nearshore stations along western U.S.A.: Predictable upwelling with the lunar cycle. *Cont. Shelf Res.*, 15: 1023-1041.
- Pingree R.D., G.T. Mardell and A.L. New. – 1986. Propagation of internal tides from the upper slopes of the Bay of Biscay. *Nature*, 321: 154-158.
- Prinsenberg S.J. and M. Rattray. – 1975. Effects of continental slope and variable Brunt-Väisälä frequency on the coastal generation of internal tides. *Deep-Sea Res.*, 22: 251-263.
- Prinsenberg S.J., W.L. Wilmot and M. Rattray. – 1974. Generation and dissipation of coastal internal tides. *Deep-Sea Res.*, 21: 263-281.
- Siedler G. and U. Paul. – 1991. Barotropic and baroclinic tidal currents in the eastern basins of the North Atlantic. *J. Geophys. Res.*, 96: 22,259-22,271.

